

Nonequilibrium steady-state response of a nematic liquid crystal under simple shear flow and electric fields

Jaka Fajar Fatriansyah, Yuji Sasaki, and Hiroshi Orihara

Division of Applied Physics, Faculty of Engineering, Hokkaido University, Sapporo, Hokkaido 060-8628, Japan

(Received 17 June 2014; published 19 September 2014)

The effect of a dc electric field on the response of a nematic liquid crystal under shear flow has been investigated by measuring the shear stress response to an ac electric field used as a probe. It was found that both the first- and second-order responses do not vanish at high frequencies, but have constant nonzero values. The experimental results are in good agreement with calculations based on the Ericksen-Leslie theory. The role of the Parodi relation (which is derived from the Onsager reciprocal relation) in the stress response is discussed.

DOI: [10.1103/PhysRevE.90.032504](https://doi.org/10.1103/PhysRevE.90.032504)

PACS number(s): 83.80.Xz, 05.70.-a, 05.40.-a

I. INTRODUCTION

Nematic liquid crystals (NLCs) can be easily taken to nonequilibrium states by applying external forces, so they have been widely used to investigate various types of nonequilibrium phenomena. Here, we confine ourselves to a nonequilibrium steady state (NESS), in which there are still many fascinating phenomena. NESSs are an interesting subject for study in general, because some theoretical results are similar to ones for the equilibrium state (ES). For example, in some cases the fluctuation-dissipation theorem (FDT) in the ES can be modified to hold in an NESS [1–6]. It should also be noted that the linear response to an external force and the correlation function of fluctuations can be defined in an NESS as well as in the ES. In an NESS of an NLC, brought about by a steady shear flow, Fatriansyah *et al.* [7] calculated the correlation function and the response function of the director orientation on the basis of a hydrodynamic theory of NLCs, called the Ericksen-Leslie (EL) theory, and derived a modified FDT, assuming that the director is independent of position, that is, the monodomain case. In this system nonconservative forces are induced by the rotational flow, which violate the usual FDT.

Experimentally, the response function in the sheared NLC was obtained by applying a small ac electric field to measure the corresponding shear stress response [8]. A characteristic response, which originated from the nonconservative force, was clearly observed. In this paper, we investigate both theoretically and experimentally the influence of a dc electric field on the shear stress response in addition to the shear flow, where a small ac electric field is also used as a perturbation probe. The dc electric field is expected to change the steady orientation of the director, bringing about qualitative changes in response. In our previous paper, it was found that the stress response would take a nonzero value, even at infinite frequency, if there is no Parodi relation, which is derived from Onsager's reciprocity. That is, the response can go to zero at infinite frequency thanks to the Parodi relation. In the following section we theoretically show that the shear stress response never vanishes at infinite frequency in the monodomain model under dc electric fields. In Sec. III, we present experimental results for the NLC 4-*n*-pentyl-4'-cyanobiphenyl (5CB) and compare them with the theoretical predictions. The last section is devoted to a summary.

II. THEORETICAL CALCULATION BASED ON EL THEORY

NLCs are composed of rodlike molecules with the long axes aligned statistically parallel to each other. The average orientation of molecules is represented by a unit vector \mathbf{n} which is called the director. Ericksen and Leslie have formulated a continuum theory for the velocity \mathbf{v} and the director \mathbf{n} of NLCs [9–14]. Hereafter, we assume a monodomain (i.e., the director is independent of position) and a simple shear flow. Under these assumptions, the EL equations can be simplified and we need only the following equations for our purpose. The angular momentum balance gives

$$\mathbf{n} \times \mathbf{h} = \gamma_1 \mathbf{n} \times \mathbf{N} + \gamma_2 \mathbf{n} \times \mathbf{A} \mathbf{n}, \quad (1)$$

where \mathbf{h} is the molecular field, \mathbf{N} is the rate of change of the director with respect to the background fluid, and $A = 1/2(\nabla_\beta v_\alpha + \nabla_\alpha v_\beta)$ is the symmetric part of the velocity gradient. The parameters γ_1 and γ_2 are the rotational and irrotational viscosity coefficients. The components of the molecular field \mathbf{h} are given by

$$h_\alpha = -\frac{\partial f}{\partial n_\alpha}, \quad (2)$$

where f is the free energy density. When subjected to an electric field, the free energy density can be written as

$$f = -\frac{1}{2}\varepsilon_0\varepsilon_\perp E^2 - \frac{1}{2}\varepsilon_0\Delta\varepsilon(\mathbf{n} \cdot \mathbf{E})^2, \quad (3)$$

where ε_0 is the dielectric constant in a vacuum, and $\Delta\varepsilon$ is the dielectric anisotropy defined as $\Delta\varepsilon = \varepsilon_{//} - \varepsilon_\perp$ with $\varepsilon_{//}$ and ε_\perp being the dielectric constants parallel and perpendicular to the director, respectively ($\Delta\varepsilon = 11.5$ for 5CB [15]). The rate of change of the director is defined as

$$N_\alpha = \frac{dn_\alpha}{dt} - W_{\alpha\beta}n_\beta, \quad (4)$$

where $W_{\alpha\beta} = 1/2(\nabla_\beta v_\alpha - \nabla_\alpha v_\beta)$ is the antisymmetric part of the velocity gradient. The constitutive equation for the viscous stress tensor is

$$\begin{aligned} \sigma_{\alpha\beta}^{(\text{visc})} = & \alpha_4 A_{\alpha\beta} + \alpha_1 n_\alpha n_\beta n_\mu n_\rho A_{\mu\rho} + \alpha_5 n_\alpha n_\mu A_{\mu\beta} \\ & + \alpha_6 n_\beta n_\mu A_{\mu\alpha} + \alpha_2 n_\alpha N_\beta + \alpha_3 n_\beta N_\alpha, \end{aligned} \quad (5)$$

where α_i ($i = 1, \dots, 6$) are Leslie coefficients, in terms of which γ_1 and γ_2 are expressed as $\gamma_1 = \alpha_3 - \alpha_2$ and

$\gamma_2 = \alpha_6 - \alpha_5$. For 5CB these coefficients have been determined [16]: $\alpha_1 = -0.00767$ Pa s, $\alpha_2 = -0.08171$ Pa s, $\alpha_3 = -0.00433$ Pa s, $\alpha_4 = 0.06642$ Pa s, $\alpha_5 = 0.06725$ Pa s, $\alpha_6 = -0.01879$ Pa s at 25 °C. These values are used in numerical calculations later. Note that, here, an NLC is treated as an incompressible fluid.

In reality, the monodomain and simple shear flow assumptions may not be exactly satisfied for various reasons. For example, in our experiment no surface treatment for aligning molecules is made so that the director and flow are spatially disturbed at least near the surfaces. Note that our model also does not accommodate defects (e.g., disclinations). Furthermore, larger deformations from the flow-aligning state are reported to take place [17]. For simplicity, however, we adopt the assumptions shown in Fig. 1(a), where $\mathbf{n}(t) = (\cos \theta, 0, \sin \theta)$ and $\mathbf{v} = \dot{\gamma} z \hat{x}$ with $\dot{\gamma}$ and \hat{x} being the shear rate and the unit vector along the x axis, respectively.

Here, we calculate the stress change due to a small ac electric field in the steady state under constant shear flow and dc electric fields. In this case, the total electric field in Eq. (3) is given as $E(t) = E_0 + \Delta E \cos \omega t$. Using Eqs. (2) and (4), Eq. (1) becomes

$$\gamma_1 \frac{\partial \theta}{\partial t} = -\frac{1}{2} \dot{\gamma} (\gamma_1 + \gamma_2 \cos 2\theta) + \frac{1}{2} \varepsilon_0 \Delta \varepsilon E(t)^2 \sin 2\theta, \quad (6)$$

where the electric field is applied in the z direction. Without the ac electric field, that is, in the nonperturbed state, the flow

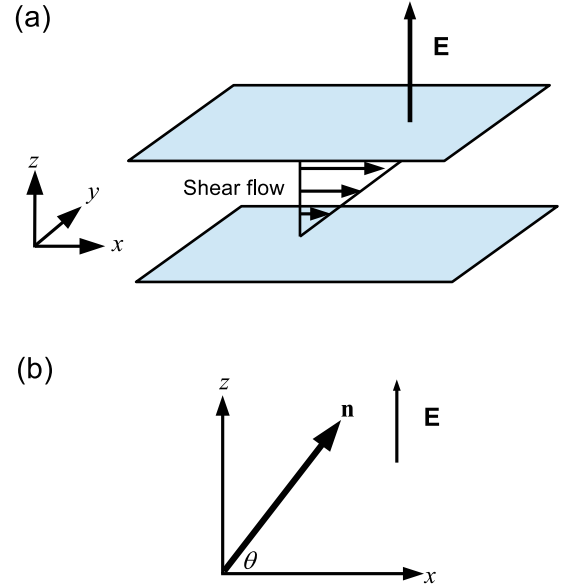


FIG. 1. (Color online) (a) A simple shear flow is applied along the x axis with a velocity gradient parallel to the z axis. An electric field is applied along the z direction. (b) We define θ to be the angle between the director and the x axis when the electric field is applied.

alignment angle θ_0 (as shown in Fig. 1) in the steady state is given as [18]

$$\theta_0 = \cos^{-1} \sqrt{\frac{(\varepsilon_0 \Delta \varepsilon E_0^2)^2 - \gamma_1 \gamma_2 \dot{\gamma}^2 + \gamma_2^2 \dot{\gamma}^2 - \sqrt{(\varepsilon_0 \Delta \varepsilon E_0^2)^2 [(\varepsilon_0 \Delta \varepsilon E_0^2)^2 + (\gamma_1^2 - \gamma_2^2) \dot{\gamma}^2]}}{2[(\varepsilon_0 \Delta \varepsilon E_0^2)^2 + \gamma_2^2 \dot{\gamma}^2]}}. \quad (7a)$$

In the special case of $E_0 = 0$, θ_0 reduces to

$$\theta_0 = \frac{1}{2} \cos^{-1} \left(-\frac{\gamma_1}{\gamma_2} \right). \quad (7b)$$

The angle θ_0 monotonically increases with increasing electric field, as shown in Fig. 2 where the values of the viscosities and the dielectric anisotropy for 5CB at 25 °C, corresponding to the experimental conditions, are used. Expanding θ up to the second order with respect to ΔE , we obtain the corresponding change in θ :

$$\Delta \theta(t) = \Delta \theta_{2,0} + \text{Re}[\Delta \theta_{1,1} e^{i\omega t}] + \text{Re}[\Delta \theta_{2,2} e^{i2\omega t}], \quad (8)$$

with

$$\Delta \theta_{1,1}(\omega) = -\frac{\varepsilon_0 \Delta \varepsilon E_0 \Delta E \sin 2\theta_0}{i\omega\tau + 1} \frac{\tau}{\gamma_1}, \quad (9)$$

$$\Delta \theta_{2,2}(\omega) = \frac{(1/2)|\Delta \theta_{1,1}|^2 (\dot{\gamma} \gamma_2 \cos 2\theta_0 - \varepsilon_0 \Delta \varepsilon E_0 \sin 2\theta_0) + \Delta \theta_{1,1} \varepsilon_0 \Delta \varepsilon E_0 \Delta E \cos 2\theta_0 + \varepsilon_0 \Delta \varepsilon \Delta E^2 \sin 2\theta_0}{2i\omega\tau + 1} \frac{\tau}{\gamma_1}, \quad (10)$$

and

$$\Delta \theta_{2,0} = \Delta \theta_{2,2}(0), \quad (11)$$

where the first subscript of $\Delta \theta$ indicates the order with respect to ΔE and the second one the harmonic order. The relaxation time τ is defined by

$$\tau = -\frac{\gamma_1}{\dot{\gamma} \gamma_2 \sin 2\theta_0 + \varepsilon_0 \Delta \varepsilon E_0^2 \cos 2\theta_0}. \quad (12)$$

Next, we calculate the shear stress response. The shear stress (σ_{zx} in the present case) can be also expanded with respect to ΔE :

$$\sigma(t) = \sigma_0 + \Delta \sigma_{2,0} + \text{Re}[\Delta \sigma_{1,1}(\omega) e^{i\omega t}] + \text{Re}[\Delta \sigma_{2,2}(\omega) e^{i2\omega t}], \quad (13)$$

where σ_0 is the shear stress with no ac electric field. It should be noted that the ω response $\Delta\sigma_{1,1}(\omega)$ appears under dc electric fields, as can be seen from Eq. (9); this response vanishes for $E_0 = 0$. The stress is independent of the polarity of the electric field as NLCs are nonpolar and, therefore, the stress response depends on $E(t)^2 = E_0^2 + 2E_0\Delta E \cos\omega t + \Delta E^2/2[1 + \cos(2\omega t)]$ as shown in Eq. (6), clearly indicating that the ω response $\Delta\sigma_{1,1}(\omega)$ should emerge under dc electric fields in addition to the 2ω response $\Delta\sigma_{2,2}(\omega)$.

From Eqs. (5), (7a), and (9)–(12), the unperturbed shear stress σ_0 and the responses $\Delta\sigma_{1,1}(\omega)$, $\Delta\sigma_{2,0}$, and $\Delta\sigma_{2,2}(\omega)$ are obtained:

$$\sigma_0 = \dot{\gamma} \left[\alpha_1 \sin^2 \theta_0 \cos^2 \theta_0 + \frac{1}{2} \{ \alpha_4 + (\alpha_5 - \alpha_2) \sin^2 \theta_0 + (\alpha_3 + \alpha_6) \cos^2 \theta_0 \} \right] \sin 2\theta_0, \quad (14)$$

$$\Delta\sigma_{1,1}(\omega) = \dot{\gamma} \left[\alpha_1 \cos 2\theta_0 - \frac{1}{2} (\alpha_2 + \alpha_3) + i\omega(\alpha_3 \cos^2 \theta_0 - \alpha_2 \sin^2 \theta_0) \right] \Delta\theta_{1,1}(\omega), \quad (15)$$

$$\begin{aligned} \Delta\sigma_{2,2}(\omega) = & \frac{\dot{\gamma}}{2} \left[\alpha_1 \sin 4\theta_0 - 2(\alpha_2 + \alpha_3) \sin 2\theta_0 + 2i\omega(\alpha_3 \cos^2 \theta_0 - \alpha_2 \sin^2 \theta_0) \right] \Delta\theta_{2,2}(\omega) \\ & + \frac{\dot{\gamma}}{2} \left[\alpha_1 \cos 4\theta_0 - (\alpha_2 + \alpha_3) \cos 2\theta_0 - i\omega(\alpha_2 + \alpha_3) \sin 2\theta_0 \right] |\Delta\theta_{1,1}(\omega)|^2, \end{aligned} \quad (16)$$

$$\Delta\sigma_{2,0} = \Delta\sigma_{2,2}(0). \quad (17)$$

When we compare the above theoretical result with experimental one, the parallel-plate geometry of the rheometer which is used in our experiment should be considered. For this geometry, the apparent shear stress is given by [8]

$$\Delta\sigma^{(R)}(\omega) = \frac{4}{\dot{\gamma}_R^3} \int_0^{\dot{\gamma}_R} \Delta\sigma(\omega, \dot{\gamma}) \dot{\gamma}^2 d\dot{\gamma}, \quad (18)$$

where $\dot{\gamma}_R$ is the shear rate at the edge of the rotating disks. The numerically calculated results are presented in Sec. IV.

III. EXPERIMENT

We used the NLC 5CB (4-*n*-pentyl-4'-cyanobiphenyl; Tokyo Chemical Industry) without any further treatment. Measurements were carried out with a parallel-plate rheometer (Physica MCR300, Anton Paar) at room temperature (25 °C).

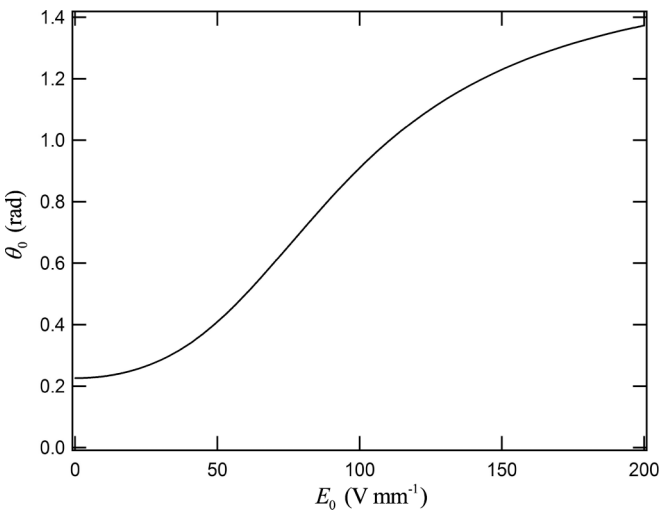


FIG. 2. E_0 dependence of θ_0 calculated from the EL theory. The angle θ_0 increases monotonically and tends to saturate when $E_0 > 200 \text{ V mm}^{-1}$.

5CB exhibits transitions from crystal to nematic phases at 18 °C and from nematic to isotropic phases at 35 °C, so we conducted experiments at 25 °C around the center of the nematic phase. The diameter of the rotating plate and the gap between the two parallel plates are 35 and 0.2 mm, respectively. In the rheometer, the shear rate is defined at the edge of the upper plate and the shear stress at the corresponding shear rate is calculated from the mechanical torque by assuming that the sample is a Newtonian fluid. Figure 1 shows the relation among the flow direction, the velocity gradient, and the electric field, which is applied to the sample by using a synthesizer (Model 1940, NF) and a high-voltage amplifier (Model 4005, NF). The experimental setup is shown in Fig. 3. The shear stress was measured with a vector signal analyzer (HP89410A, Hewlett-Packard) and the first- and second-order harmonics were obtained.

The shear stress response to ac electric field under steady shear flow and electric fields was measured by applying a small ac electric field $\Delta E \cos(\omega t)$. We obtained the first-order response $\Delta\sigma_{1,1}(\omega)$ and the second-order response $\Delta\sigma_{2,2}(\omega)$, which should be proportional to ΔE and ΔE^2 , respectively, for small ΔE . The dc electric field dependencies of the first- and second-order responses are shown in Fig. 4, where the measurements were done at $\dot{\gamma} = 10 \text{ s}^{-1}$ and $E_0 = 100 \text{ V mm}^{-1}$. Linearity was confirmed to hold at least up to $\Delta E = 20 \text{ V mm}^{-1}$. All the measurements were performed at $\Delta E = 14.1 \text{ V mm}^{-1}$ and $\dot{\gamma} = 10 \text{ s}^{-1}$.

IV. RESULTS AND DISCUSSION

First, we discuss the first-order response $\Delta\sigma_{1,1}(\omega)$ shown in Fig. 5 (lines are experimental results and dots are theoretical predictions). The first-order response appears only when we apply a dc electric field E_0 . When E_0 is low ($E_0 = 20 \text{ V mm}^{-1}$) [see Fig. 5(a)], the experimental stress response resembles Debye-type relaxation. However, as we increase E_0 to 80 V mm^{-1} [see Fig. 5(b)], we can see that the response remains nonzero even at high frequencies, forming what is

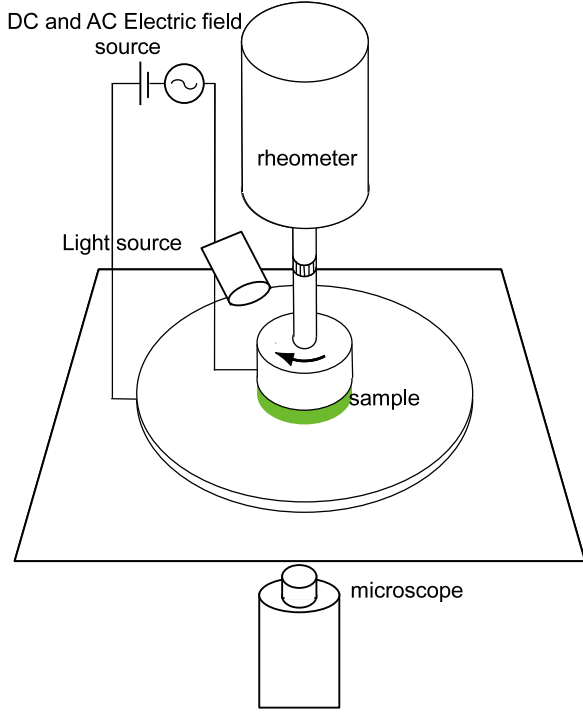


FIG. 3. (Color online) Experimental setup. Electric fields are applied between the top and bottom plates. For the electro-optical experiment we add a light source and a microscope to observe the change of transmitted intensity. (In the figure: dc and ac electric field source, microscope, sample, rheometer.)

referred to as a plateau. The emergence of the plateau is the most remarkable characteristic of the response to ac electric field under dc electric fields. From the EL theory, it is easily seen that the plateau comes from the third term with $i\omega$ in the bracket on the right-hand side of Eq. (15) because $\Delta\theta_{1,1}(\omega)$ in Eq. (15) is inversely proportional to $i\omega$ at high frequencies, as can be seen from Eq. (9). The $i\omega$ term appears as a result of differentiating the director with respect to time in Eq. (4). In the limit as $\omega \rightarrow \infty$, we have

$$\Delta\sigma_{1,1}(\infty) = \frac{\dot{\gamma}(\alpha_3 \cos^2 \theta_0 - \alpha_2 \sin^2 \theta_0)\tau}{\gamma_1} \times \varepsilon_0 \Delta\varepsilon E_0 \Delta E \sin 2\theta_0. \quad (19)$$

It should be noted that the director response $\Delta\theta_{1,1}(\omega)$ vanishes at high frequencies, but the stress response $\Delta\sigma_{1,1}(\omega)$ remains nonzero.

At higher values of E_0 , the height of the plateau is larger than at low frequencies, as shown in Figs. 5(b) (80 V mm^{-1}) and 5(c) (160 V mm^{-1}). The agreement between the experimental and theoretical results for all E_0 shown in Fig. 5 is fairly good. The dependence of plateau height $\Delta\sigma_{1,1}(\infty)$ on E_0 is shown in Fig. 6 for the experiment and the theoretical result in Eq. (15). From Fig. 6, we observe that when $E_0 < 40 \text{ V mm}^{-1}$ the plateau is small. As we increase E_0 to more than 50 V mm^{-1} , the plateau height increases sharply. In the same figure, we also plot the E_0 dependencies of $\Delta\sigma_{1,1}$ calculated at zero frequency and experimentally obtained from Fig. 5 at 0.23 rad s^{-1} . The agreement between them is good. The low-frequency and high-frequency (plateau)

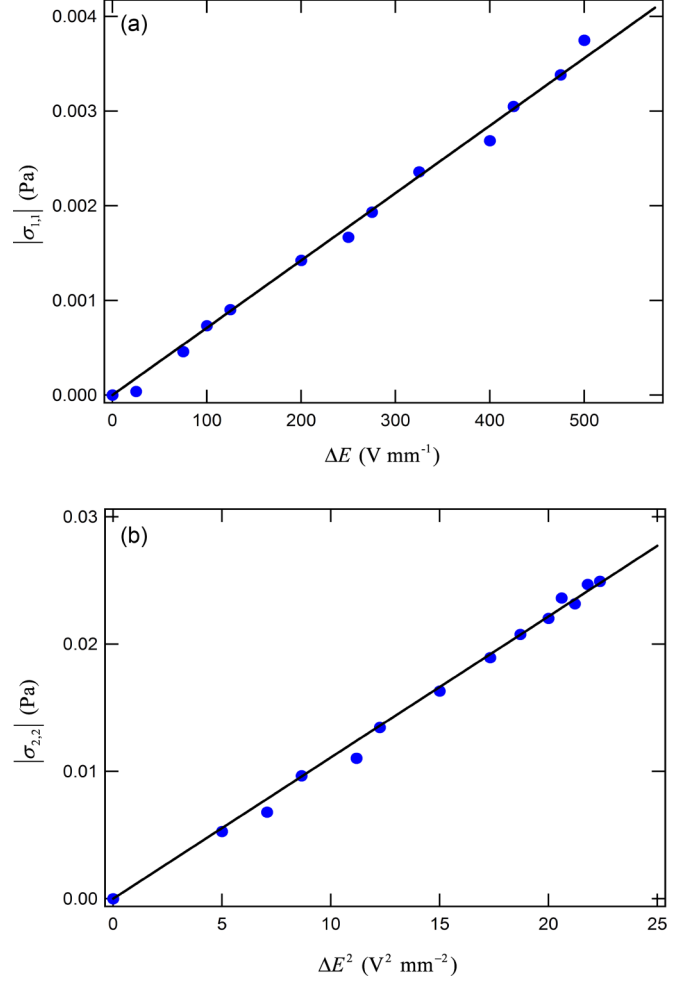


FIG. 4. (Color online) Dependence of $|\sigma_{1,1}|$ on ΔE (a) and $|\sigma_{2,2}|$ on ΔE^2 (b) at $\dot{\gamma} = 10 \text{ s}^{-1}$ and $E_0 = 100 \text{ V mm}^{-1}$. Linear relations are obtained at low ac electric fields.

values exchange at around $E_0 = 90 \text{ V mm}^{-1}$. The imaginary part of the response (Fig. 5) goes to zero at both low and high frequencies, and shows good agreement between theory and experiment. The peak or valley frequency of the imaginary part is seen to increase with increasing dc electric field, though it changes sign from positive to negative at around $E_0 = 90 \text{ V mm}^{-1}$ corresponding to the above-mentioned exchange of the low- and high-frequency values of the response.

Next, let us discuss the second-order response $\Delta\sigma_{2,2}$ (Fig. 7). This response is more complicated than the first-order response since there are contributions from the first-order mode $\Delta\theta_{1,1}$ as well as $\Delta\theta_{2,2}$, as can be seen from Eq. (16). It should be noted that the second-order response appears even without a dc electric field, as shown in Fig. 7(a). The stress response resembles Debye-type relaxation for $E_0 = 0$. However, one may notice that the real part becomes slightly negative at around 10 rad s^{-1} . We have previously observed this negative part and shown that it originates from nonconservative forces due to the shear flow [8]. This is a remarkable characteristic of nonequilibrium steady states of systems under shear flow and is observed also in an immiscible polymer blend in which one polymer is dispersed as droplets

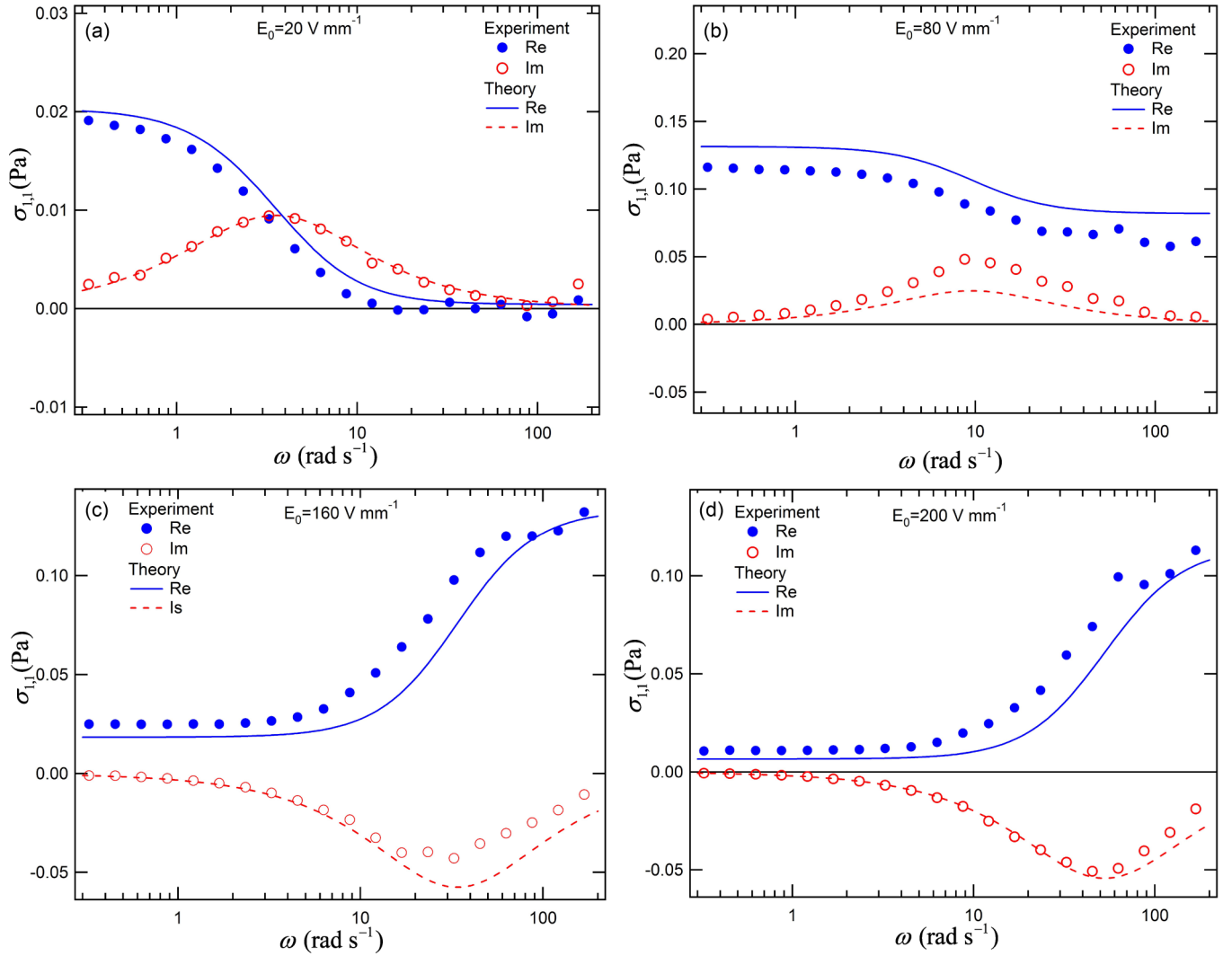


FIG. 5. (Color online) Frequency dispersion of $\Delta\sigma_{1,1}$ as a function of angular frequency ω . The theoretical curves are obtained from Eq. (15). A characteristic nonzero plateau, which is due to the dc electric field, appears at high frequencies in (b)–(d).

in the other [19]. The nonconservative forces also violate the fluctuation-dissipation relation (FDR). Fatriansyah *et al.* have theoretically clarified the mechanism of the appearance of the nonconservative forces in NLCs and derived a modified FDR [7]. According to the theory, the nonconservative forces can emerge only when the director is out of the shear plane. In Sec. II, however, we assumed that the director is confined in the shear plane and, therefore, we cannot reproduce the negative part in the present model. The director may tend to be in the shear plane under a dc electric field. Therefore, it is expected that our monodomain model works better as the dc electric field is increased.

From Fig. 7, it is obvious that there is a plateau at every dc electric field except for $E_0 = 0$ [Fig. 7(a)]. As we increase E_0 , the plateau, which is the characteristic of the system under dc electric fields, appears. The origin of the plateau in the second-order response is the same as that in the first-order response. The plateau comes from the ω term proportional to $\Delta\theta_{2,2}$ in Eq. (16), which includes a factor $(\alpha_3 \cos^2 \theta_0 - \alpha_2 \sin^2 \theta_0)$. This factor also appears in the ω term of the first-order response [see Eq. (15)]. Interestingly, this vanishes at $E_0 = 0$ due to the

Parodi relation $\alpha_6 - \alpha_5 = \alpha_2 + \alpha_3$, which is easily proved by using Eq. (7b). Note that the second-order response does not vanish for $E_0 = 0$ unlike the first-order response. It is obvious that the factor is in general not zero for $E_0 \neq 0$. When we increase E_0 to 80 V mm^{-1} , the plateau at high frequencies rises, as shown in Fig. 7(b). The plateau becomes remarkable for $E_0 = 120 \text{ V mm}^{-1}$ [Fig. 7(d)]. The agreement between the experimental and theoretical results is good. The imaginary part of the response also shows good agreement between theory and experiment.

Figure 8 shows the E_0 dependence of $\Delta\sigma_{2,2}$ calculated at zero frequency and experimentally obtained from Fig. 7 at 0.23 rad s^{-1} . Also in the same figure we show the E_0 dependence of the height of the plateau. Good agreement is obtained between the theory and experiment. The E_0 dependencies are more complicated than those in the first-order response.

Finally, we show experimental evidence that the plateau observed in the real part of the first-order response should be ascribed to the time derivative of the director, but not to $\Delta\theta_{1,1}$ itself. To do so, we made an optical measurement using crossed

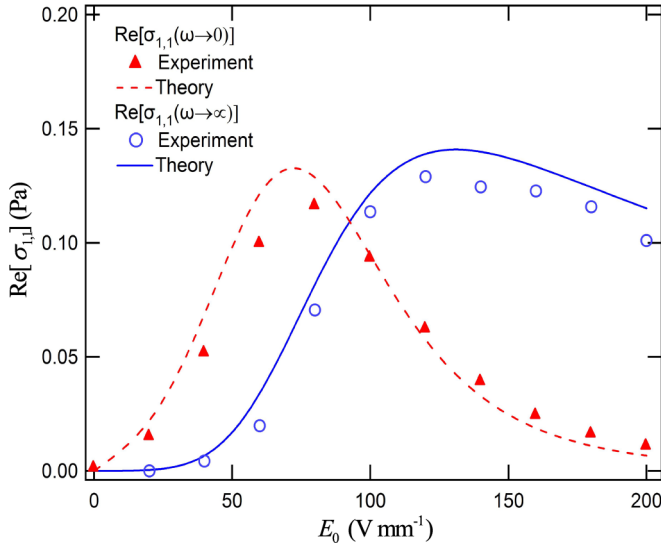


FIG. 6. (Color online) E_0 dependence of the first-order response at very low frequency (0.23 rad s^{-1} for the experiment and exactly zero for the theory), $\text{Re}[\Delta\sigma_{1,1}(\omega \rightarrow 0)]$. Also shown is the dependence of plateau height $\text{Re}[\Delta\sigma_{1,1}(\omega \rightarrow \infty)]$. For dc electric fields higher than around 90 V mm^{-1} , $\text{Re}[\Delta\sigma_{1,1}(\omega \rightarrow \infty)]$ becomes larger than $\text{Re}[\Delta\sigma_{1,1}(\omega \rightarrow 0)]$.

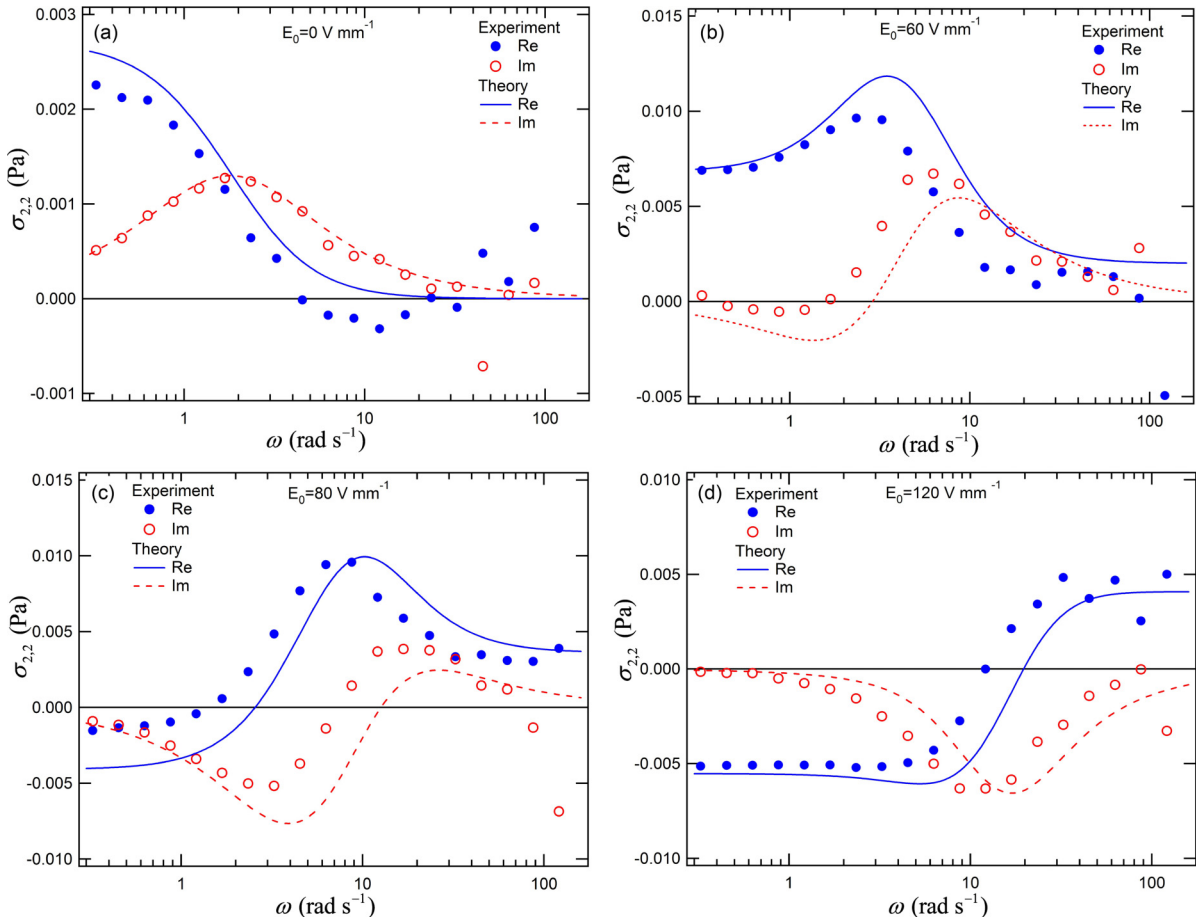


FIG. 7. (Color online) Frequency dispersion of $\Delta\sigma_{2,2}$ as a function of angular frequency ω . The theoretical curves are obtained from Eq. (16). A plateau appears under dc electric fields as well as in the first-order response.

polarizers, in which the light intensity is shown to be just proportional to the first-order mode $\Delta\theta_{1,1}$. Therefore, if $\Delta\theta_{1,1}$ is of the Debye type, there should be no plateau observed in the optical response at high frequencies, though it is observed in the shear stress response.

When an electric field is applied, the birefringence $n_a(\theta) = n_e(\theta) - n_0(\theta)$, where n_0 and n_e are the ordinary and extraordinary refractive indices, respectively, will change and here the observation is assumed to be made perpendicular to the parallel plates as shown in Fig. 3. In NLCs, n_0 is independent of the director orientation θ . However, $n_e(\theta)$ is dependent on θ :

$$n_e(\theta) = \frac{n_{\perp}n_{\parallel}}{(n_{\perp}^2 \cos^2 \theta + n_{\parallel}^2 \sin^2 \theta)^{1/2}} - n_{\parallel}, \quad (20)$$

where n_{\parallel} and n_{\perp} are the refractive indices parallel and perpendicular to the director. On the other hand, the transmitted light intensity of the NLC under crossed polarizers is given by

$$I = I_0 \sin^2(2\alpha) \sin^2 \frac{\pi n_a(\theta) d}{\lambda}, \quad (21)$$

where I_0 is the incoming light intensity, α is the angle between the polarizer and the x axis, d is the sample thickness, and λ is the wavelength of the light in a vacuum. For a small change of θ , $\Delta\theta$, due to the application of an ac electric field, the corresponding change of I , ΔI , is obtained from Eqs. (20)

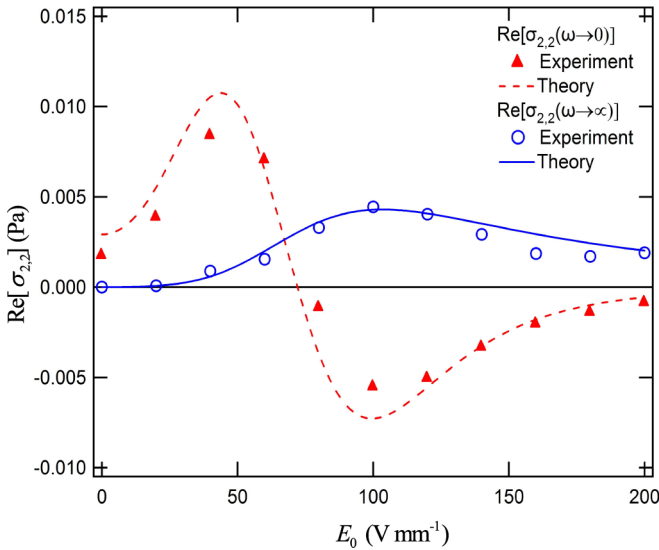


FIG. 8. (Color online) E_0 dependence of the first-order response at a very low frequency (0.23 rad s^{-1} for the experiment and exactly zero for the theory), $\text{Re}[\Delta\sigma_{2,2}(\omega \rightarrow 0)]$. Also shown is the dependence of plateau height $\text{Re}[\Delta\sigma_{2,2}(\omega \rightarrow \infty)]$.

and (21):

$$\Delta I = I_0 \sin^2(2\alpha) \sin^2 \left[\frac{\pi n_a(\theta_0) d}{\lambda} \right] \times \frac{n_{\perp} n_{\parallel} (n_{\perp}^2 - 2n_{\parallel}^2 \cos^2 \theta_0) \sin \theta_0}{2(n_{\perp}^2 \cos^2 \theta_0 + n_{\parallel}^2 \sin^2 \theta_0)^{3/2}} \Delta\theta, \quad (22)$$

where θ_0 is the angle without any ac electric field.

In the optical measurement we replaced the upper plate by a glass disk with diameter 40 mm so that we could observe the transmitted light through the sample. As a light source we used a halogen lamp (LS-LHA, Sumita Optical Glass). The light intensity was converted by a photosensor into a voltage and it was amplified (C6386, Hamamatsu Photonics).

The experimental result is shown in Fig. 9 for $E_0 = 200 \text{ V mm}^{-1}$. Note that the vertical axis is adjusted so that the theoretical and experimental results coincide as well as possible, because it is difficult to determine the coefficient in Eq. (22). The agreement between the experiment and theory is good, though the data are scattered to some degree. The relaxation frequency experimentally observed is in good agreement with the one theoretically obtained. There is no plateau in the optical response, in contrast to the stress response, convincing us that the plateau observed in the stress response should originate from the time derivative of the director.

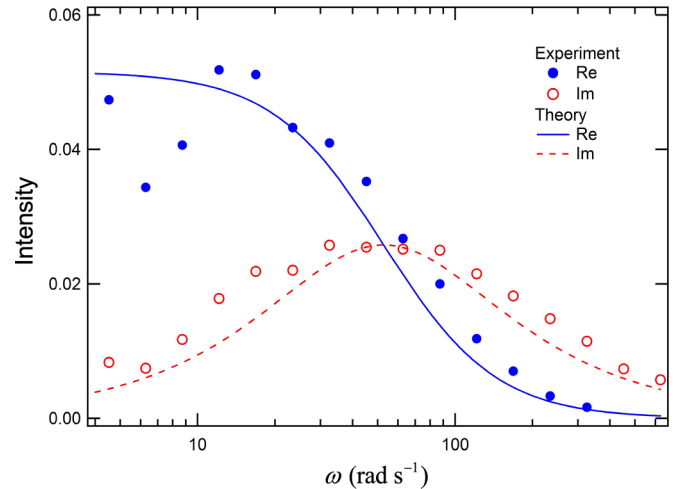


FIG. 9. (Color online) Frequency dispersion of the optical response, which corresponds to the director response, as a function of angular frequency ω . Lines are the experiment and circles are the theory. No plateau is observed, which shows that the plateau observed in the shear stress response should be ascribed to the time derivative of the director but not to $\Delta\theta_{1,1}$ itself.

V. SUMMARY

We have investigated the NESS response of an NLC to an ac electric field under constant dc electric field and steady shear flow. The first- and second-order shear stress responses were theoretically obtained from the EL theory assuming a monodomain model. It was found theoretically and experimentally that when we apply a dc electric field both responses remain constant and nonzero even at high ac electric field frequencies. That is, there is a plateau, which originates from the time derivative of the director. This plateau is a remarkable feature in the shear stress response brought about by the application of a dc electric field. Furthermore, by performing an optical measurement, the director response is confirmed to vanish at high frequencies, strongly supporting the above-mentioned mechanism for the appearance of the plateau. It was also clarified that the plateau in the second-order response disappears in the absence of a dc electric field, due to the Parodi relation, which is derived from the Onsager reciprocal relation.

ACKNOWLEDGMENTS

This work was supported by Grant-in-Aids for Scientific Research on Innovative Areas “Fluctuation & Structure” (No. 25103006) and for Scientific Research (B) (No. 26289032) from the Ministry of Education, Culture, Sports, Science, and Technology of Japan.

- [1] T. Sakaue and T. Ohta, *Phys. Rev. E* **77**, 050102 (2008).
- [2] J. R. Gomez-Solano, A. Petrosyan, S. Ciliberto, R. Chetrite, and K. Gawedzki, *Phys. Rev. Lett.* **103**, 040601 (2009).
- [3] J. Mehl, V. Blickle, U. Seifert, and C. Bechinger, *Phys. Rev. E* **82**, 032401 (2010).

- [4] U. Seifert and T. Speck, *Europhys. Lett.* **89**, 10007 (2010).
- [5] H. D. Feng and J. Wang, *J. Chem. Phys.* **135**, 234511 (2011).
- [6] D. Chaudhuri and A. Chaudhuri, *Phys. Rev. E* **85**, 021102 (2012).
- [7] J. F. Fatriansyah and H. Orihara, *Phys. Rev. E* **88**, 012510 (2013).

- [8] H. Orihara, F. Yang, Y. Takigami, Y. Takikawa, and Y. H. Na, [Phys. Rev. E](#) **86**, 041701 (2012).
- [9] J. L. Ericksen, [Trans. Soc. Rheol.](#) **11**, 5 (1967).
- [10] F. M. Leslie, [Arch. Rational Mech. Anal.](#) **28**, 265 (1968).
- [11] O. Parodi, [J. Phys. France](#) **31**, 581 (1970).
- [12] F. M. Leslie, [Rheol. Acta](#) **10**, 91 (1971).
- [13] P. G. de Gennes and J. Prost, *The Physics of Liquid Crystals* (Clarendon, Oxford, UK, 1993).
- [14] S. Chandrasekhar, *Liquid Crystals*, 2nd ed. (Cambridge University Press, Cambridge, UK, 1992).
- [15] P. G. Cummins, D. A. Dunmur, and D. A. Laidler, [Mol. Cryst. Liq. Cryst.](#) **30**, 109 (1975).
- [16] G. Ahlers, *Pattern Formation in Liquid Crystals*, edited by L. Kramer and A. Buka (Springer, Berlin, 1996).
- [17] T. Tsuji and A. D. Rey, [Phys. Rev. E](#) **57**, 5609 (1998).
- [18] K. Negita, [J. Chem. Phys.](#) **105**, 7837 (1996).
- [19] Y. H. Na, K. Aida, R. Sakai, T. Kakuchi, and H. Orihara, [Phys. Rev. E](#) **80**, 061803 (2009).